Optimized Rotations for LDPC-coded MPSK Constellations with Signal Space Diversity

Nauman F. Kiyani, Umar H. Rizvi, Jos H. Weber and Gerard J. M. Janssen

IRCTR/CWPC, Wireless and Mobile Communications Group,

Faculty of Electrical Engineering, Mathematics and Computer Science,

Delft University of Technology, Delft, the Netherlands.

Email(s): {n.f.kiyani, u.h.rizvi, j.h.weber, g.janssen}@ewi.tudelft.nl

Abstract— **For multi-level modulation methods, rotation of the signal constellation together with in-phase and quadrature phase channel interleaving (signal space diversity) are known to provide good performance gains over fading channels. This paper studies the extension of such schemes with a low density parity check (LDPC) code. It is shown that for both coded and uncoded Gray-mapped MPSK modulation formats with signal space diversity on a Rayleigh fading channel, a well-considered choice of the rotation angle may lead to a significant gain over the conventional unrotated constellation. However, the optimum rotation angle for the coded scheme may be different from the corresponding optimization angle of the uncoded scheme.**

I. INTRODUCTION

The research for next generation wireless communication systems is oriented towards the development of efficient transmission techniques through band-limited communication channels at lower signal-to-noise ratios. Diversity coupled with coding has been proposed as one of the options. In this paper, we present the use of practically sized low density parity check (LDPC) codes in combination with signal space diversity to achieve gain in band-limited wireless communication systems. LDPC codes with message passing algorithms have achieved excellent performance over additive white Gaussian noise (AWGN) channels [1]. Their potential as capacity achieving codes for more realistic wireless channels has not been established yet. Preliminary results are available which suggest that they can achieve capacity for a wide range of channels [2]. Fading causes significant performance degradation in wireless digital communication systems. For block fading channels, improved performance can be obtained by the use of coded modulation techniques coupled with interleaving [3].

It was argued that maximizing the minimum squared Euclidean distance does not necessarily minimize the error probability over fading channels [3]. Therefore, an optimum scheme for an AWGN channel may not be the best possible solution for a fading channel. It was shown in [4], [5] that for a block fading wireless communication link, diversity can be introduced into the system by separately interleaving the in-phase and quadrature components of a QPSK scheme and performing symbol-by-symbol detection. The performance of such a scheme was shown to be dependent upon the constellation rotation angle and is not effected when employed in an AWGN channel. Furthermore, in [6], [7] it was shown that iterative decoding can increase the minimum intersignal

Euclidean distance of bit interleaved coded modulation, while retaining the desirable Hamming distance. It allows for an indirect translation of large Hamming distance to large free Euclidean distance when the signal labeling is carefully designed.

The idiosyncracy of LDPC codes is that if the noise level is smaller than a certain noise threshold, the bit error probability goes to zero as the block size reaches infinity and the codes approach channel capacity [1]. However, these codes have too high complexity to be considered for real-time applications. Random, regular incarnations of LDPC codes provide an alternative where the complexity and the size are reduced with a loss in performance [8]. In this paper, we present regular, random LDPC codes coupled with signal space diversity and Gray-mapped multi-level modulation schemes in a block uncorrelated Rayleigh fading channel. To maximize the diversity order, the constellation of an MPSK signal should be properly rotated such that all distinct symbols are separable on every coordinate [4]. A symbol to bit de-mapper for multi-level modulation schemes with signal space diversity is introduced and Gray-mapped, uncoded and LDPC-coded QPSK and 8PSK constellations under various rotation angles are considered.

Section II introduces the system model and outlines the main blocks. LPDC-coded signal space diversity employing Gray-mapping is presented in Section III . The performance curves of the new concatenated scheme are presented in Section IV, followed by conclusions in Section V.

II. SYSTEM MODEL

The block diagram of an LDPC-coded system with signal space diversity is shown in Figure 1. The encoded bits are mapped onto symbols using rotated signal constellations which are assumed to be Gray-mapped. The I and Q components of the mapped symbols are then separately interleaved and transmitted through the Rayleigh fading channel which is assumed to be block independent. The I and Q interleavers uncorrelate the in-phase and quadrature components. At the receiver, the received in-phase and quadrature components are de-interleaved. The de-interleaved components along with the channel state information (CSI) are utilized by the symbol to bit de-mapper which generates intrinsic log likelihood ratios (LLR) for LDPC decoding.
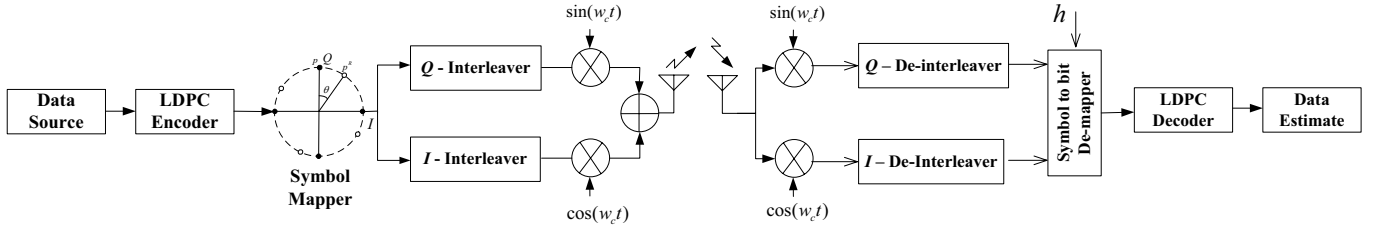
Fig. 1.   System Model

The next subsections describe the various blocks in more detail. The specific decoding aspects of the LDPC code in this scheme are further discussed in Section III.

A. Rotated MPSK Constellations

A conventional M-ary phase-shift keying (MPSK) signal constellation is denoted by $\mathcal{S}_M = \{s_k = e^{2\pi(k/M)j} : k = 0, 1, \ldots, M-1\}$, where the energy has been constrained to unity. Clockwise rotation over an angle θ (see Figure 2) leads to the constellation

$$\mathcal{S}_M^\theta = \{s_k = e^{(2\pi(k/M)-\theta)j} : k = 0, 1, \ldots, M-1\}. \quad (1)$$

Such a (complex) modulation scheme can be seen as two (real) M-ary pulse amplitude modulations (MPAMs) in parallel – one on the in-phase (I channel) and the other on the quadrature channel (Q channel). For the QPSK and 8PSK constellations under consideration in this paper, the symbol representations and the associated bit-maps are given in Table I.
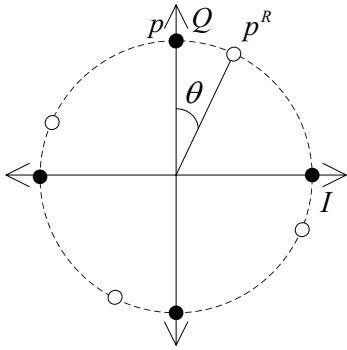

Fig. 2.   Signal constellation rotation

B. Separate I and Q Component Interleaving

It was shown in [4], [5] that by rotating the signal constellation and separately interleaving the I and Q components, an improved performance can be obtained for a QPSK system without effecting its bandwidth efficiency. In case of transmission of N symbols, each taken from the rotated constellation $\mathcal{S}_M^\theta$, let the sequence of I components $x = (x_0, x_1, \ldots, x_{N-1})$ and the sequence of Q components $y = (y_0, y_1, \ldots, y_{N-1})$ be interleaved by the I interleaver η and the Q interleaver ρ, respectively, resulting in the sequences $\tilde{x} = \eta(x) =$

$(\tilde{x}_0, \tilde{x}_1, \ldots, \tilde{x}_{N-1})$ and $\tilde{y} = \rho(y) = (\tilde{y}_0, \tilde{y}_1, \ldots, \tilde{y}_{N-1})$. The transmitted waveform for the rotated and interleaved system is given by

$$
\begin{aligned}
s(t) &= \sum_{i=0}^{N-1} \tilde{x}_i p(t - iT_s) \cos(2\pi f_c t) \\
&+ \sum_{i=0}^{N-1} \tilde{y}_i p(t - iT_s) \sin(2\pi f_c t).
\end{aligned}
\quad (2)
$$

where

$$p(t) = \begin{cases} 1, & 0 \le t \le T_s, \\ 0, & \text{otherwise}, \end{cases}$$

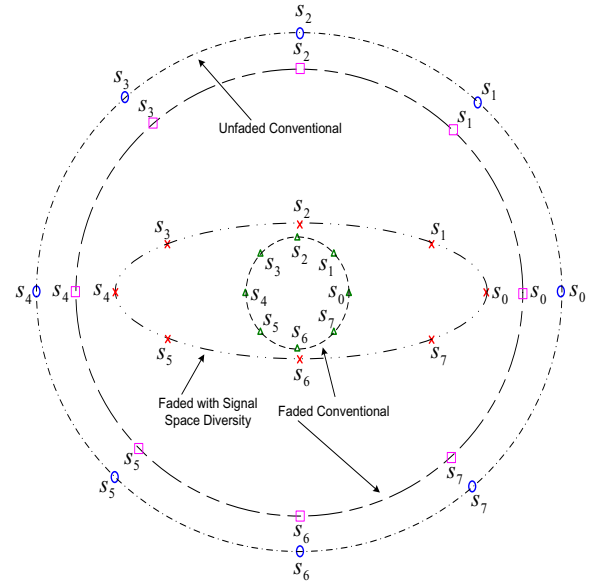T_s is the symbol period and f_c is the carrier frequency.

Fig. 3.   Conventional 8PSK constellation under channel fading.

C. Rayleigh Fading

It is assumed that the transmission is over a block independent Rayleigh fading channel with perfect CSI available at the receiver. Under these assumptions the baseband input/output relation per channel use is given by

$$
\begin{aligned}
\tilde{r}_i^I &= \tilde{h}_i \tilde{x}_i + \tilde{n}_i^I, \\
\tilde{r}_i^Q &= \tilde{h}_i \tilde{y}_i + \tilde{n}_i^Q,
\end{aligned}
\quad (3)
$$

TABLE I

SYMBOL REPRESENTATIONS AND BIT-MAPS FOR UNROTATED QPSK AND 8PSK CONSTELLATIONS.

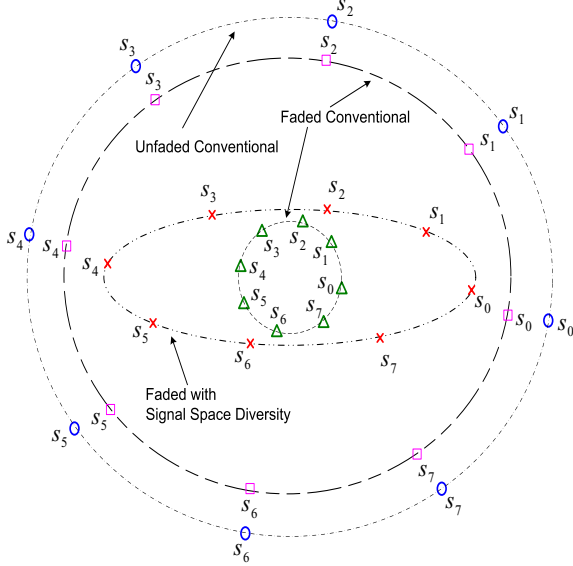| **QPSK** symbols	$s_0 = 1$	$s_1 = j$	$s_2 = -1$	$s_3 = -j$			
I,Q representation	$(1,0)$	$(0,1)$	$(-1,0)$	$(0,-1)$			
bit-map (Gray)	00	01	11	10			
8PSK symbols	$s_0 = 1$	$s_1 = e^{j\pi/4}$	$s_2 = j$	$s_3 = e^{3j\pi/4}$	$s_4 = -1$	$s_5 = e^{5j\pi/4}$	$s_6 = -j$	$s_7 = e^{7j\pi/4}$
I,Q representation	$(1,0)$	$(\sqrt{1/2}, \sqrt{1/2})$	$(0,1)$	$(-\sqrt{1/2}, \sqrt{1/2})$	$(-1,0)$	$(-\sqrt{1/2}, -\sqrt{1/2})$	$(0,-1)$	$(\sqrt{1/2}, -\sqrt{1/2})$
bit-map (Gray)	000	001	011	010	110	111	101	100

Fig. 4.   Rotated 8PSK constellation under channel fading.

where the $\tilde{h}_i$ are normalized and independent *Rayleigh fading factors* with $\mathcal{E}\left[(\tilde{h}_i)^2\right] = 1$ and probability density function $p(\alpha) = 2\alpha e^{-\alpha^2}, \alpha > 0$, and $\tilde{n}_i^I$ and $\tilde{n}_i^Q$ are independent and identically distributed (i.i.d) Gaussian random variables with zero mean and variance $N_0/2$. Separate interleaving of I and Q components thus results for each symbol in transmitting the I component x_i during one fade interval and the Q component y_i during another fade interval. This kind of interleaving adds diversity in the system as x_i and y_i experience independent fading.

D. Symbol Detection

De-interleaving the received sequences $\tilde{r}^I$ and $\tilde{r}^Q$ results in the sequences $r^I = \eta^{-1}(\tilde{r}^I)$ and $r^Q = \rho^{-1}(\tilde{r}^Q)$. We assume that perfect CSI is available, i.e., the fading sequence $\tilde{h} = (\tilde{h}_0, \tilde{h}_1, \ldots, \tilde{h}_{N-1})$ and thus the de-interleaved fading component sequences $h^I = \eta^{-1}(\tilde{h})$ and $h^Q = \rho^{-1}(\tilde{h})$ are known at the receiver. For any i, the symbol $s_k = (s_k^I, s_k^Q) \in \mathcal{S}_M^\theta$ which minimizes the metric

$$\left| r_i^I - h_i^I s_k^I \right|^2 + \left| r_i^Q - h_i^Q s_k^Q \right|^2 \qquad (4)$$

is chosen as the estimate $(\hat{x}_i, \hat{y}_i)$ of (x_i, y_i).

An intuitive explanation for the benefit of signal space diversity can be given with reference to Figure 3. In a conventional system, the I and the Q components experience the same fading, which may be deep (the small circle) or only moderate (larger circle). Of course, in case of a deep-fade, the system is quite error-prone. In a system with signal space diversity, however, the I and the Q components experience different fading (indicated by the ellipse). In spite of the fact that the Q component was exposed to severe fading, the distances between the signal points on the ellipse are considerably larger than the corresponding distances of the signal points on the small circle. The possible added value of rotation becomes evident in the comparison of Figures 3 and 4, which clearly show that the symbol distance profiles on the ellipse change under rotation. The figures also show that the system with signal space diversity no longer exhibits equi-probable symbol error probabilities as is the case with the conventional 8PSK scheme. Therefore, in systems employing signal space diversity, the performance cannot be evaluated by transmitting continuously a single symbol.

III. LDPC-CODED SIGNAL SPACE DIVERSITY

The received r^I and r^Q de-interleaved components are decoded in two steps [9] as shown in Figure 1. The first step corresponds to the calculation of intrinsic LLR values by the symbol to bit de-mapper. The intrinsic LLR values are passed to an iterative LDPC decoder. The following subsections describe these blocks in more detail.

A. Symbol to Bit De-mapping for MPSK Constellations

Assuming perfect CSI, the LLR values for MPSK systems are given in [9], [10] which are modified to incorporate signal space diversity as

$$\Lambda(b_{i,m}) = \log\left(\frac{\max_{l \in \mathcal{S}_{+m}}\left\{\exp\left(E_{i,l}^1 + E_{i,l}^2\right)\right\}}{\max_{l \in \mathcal{S}_{-m}}\left\{\exp\left(E_{i,l}^1 + E_{i,l}^2\right)\right\}}\right)$$
$$= \max_{l \in \mathcal{S}_{+m}}\left\{E_{i,l}^1 + E_{i,l}^2\right\} - \max_{l \in \mathcal{S}_{-m}}\left\{E_{i,l}^1 + E_{i,l}^2\right\}, \qquad (5)$$

where in the above equation $\Lambda(b_{i,m})$ denotes the LLR value and $b_{i,m}$ is bit m of symbol i ($m = 1, 2, \ldots, \log_2 M; i = 0, 1, \ldots, N-1$). In (5), $\mathcal{S}_{+m}$ denotes the set of symbols for which the $m-$th bit is 1 and

similarly the set $\mathcal{S}_{-m}$ denotes the set of symbols for which the m−th bit is 0. $E^1_{i,l}$ and $E^2_{i,l}$ are defined as:

$$E^1_{i,l} = -\frac{1}{N_0} \left| r^I_i - h^I_i s^I_l \right|^2,$$

$$E^2_{i,l} = -\frac{1}{N_0} \left| r^Q_i - h^Q_i s^Q_l \right|^2. \tag{6}$$

The initial intrinsic LLRs computed by the symbol to bit de-mapper are passed to the LDPC decoder.

B. LDPC Decoder

One of the most widely used decoding methods for LDPC codes is based on belief propagation. It is performed by applying the maximum *a posteriori* (MAP) algorithm [1]. This algorithm aims at minimizing the bit error rate of the decoded sequence and iteratively calculates the *a posteriori* probabilities. Consider a regular (j, k) LDPC code with v as the LLR message passed from a variable node of degree j to a check node of degree k, given as [8]

$$v = \Lambda + \sum_{i=1}^{j-1} u_i, \tag{7}$$

where, Λ is *intrinsic information* passed from the symbol to bit de-mapper (5) for the variable node under consideration, and u_i, for all $i = 1, \ldots, j - 1$, is the incoming *extrinsic information* from the neighbors of the variable node except the check node that gets the message v. Extrinsic information is part of the overall LLR stemming from the observation of the received samples.

The check nodes update rule is obtained by noticing the duality between variable and check nodes. It is based upon the well known *tanh* rule and is given as [1]

$$\tanh \frac{u}{2} = \prod_{i=1}^{k-1} \tanh \frac{v_i}{2}, \tag{8}$$

where v_i, for all $i = 1, \ldots, k - 1$, are the incoming LLRs from $k - 1$ neighbors of a degree-k check node and u is the output LLR message sent to the remaining neighbors.

IV. SIMULATION RESULTS AND DISCUSSION

This section presents simulation results for conventional and rotated QPSK and 8PSK uncoded and LDPC-coded schemes employing signal space diversity. The channel dynamics are explicitly taken into account by considering a block-independent fading model. The fading is considered to be constant for a block length and independent from block to block. We use a random regular $(3, 6)$ LDPC code of length 504 and rate $\frac{1}{2}$. The $(3, 6)$ random regular LDPC code was generated as presented in [8]. Maximum of 100 iterations were performed at the LDPC decoder.

Figures 5 and 6 show the bit error rate (BER) as a function of various rotation angles for LDPC-coded and uncoded QPSK and 8PSK modulation schemes with signal space diversity for given E_b/N_0. The BER curves were simulated by transmitting randomly generated symbols and code words for a fixed

E_b/N_0 for different rotation angles. For QPSK, the angles which minimize the BER were found to be $15°$ at $E_b/N_0 = 10$ dB and $26°$ at $E_b/N_0 = 5$ dB for uncoded and LDPC-coded system, respectively. For the 8PSK constellation, the angles which minimize the BER were found to be $54°$ at $E_b/N_0 = 15$ dB and $70°$ at $E_b/N_0 = 6$ dB for uncoded and LDPC-coded systems, respectively. These angles are for Gray-mapped constellations and would vary if the mapping was to be modified. The Figures 5 and 6 show that at some rotation angles for Gray-mapped constellations the performance can be worse than the conventional (unrotated) case, as explained in Section II. Furthermore, it is quite evident from the figures that an angle providing gain in an uncoded system does not necessarily leads to a performance improvement in the coded case. It is important to note that the stated minimum BER rotation angles are for specific E_b/N_0 and for Gray-mapped constellations employing regular (3,6) LDPC code.
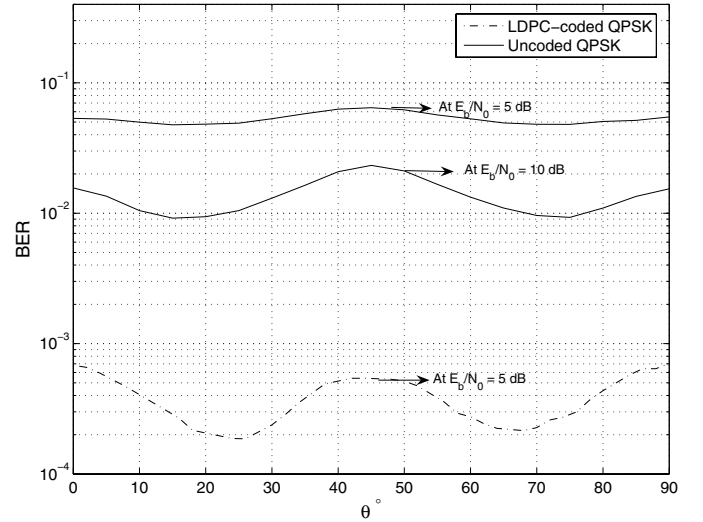

Fig. 5. BER performance of uncoded and LDPC-coded QPSK systems with signal space diversity over different rotation angles.

Figures 7 and 8 illustrate the performance gains of constellation rotation in LDPC-coded and uncoded rotated and unrotated QPSK and 8PSK modulation schemes. Figure 7 shows that rotated LDPC coded systems have a gain of 0.31 dB at BER of 5×10^{-4} over the unrotated case. Similarly for an uncoded case this improvement is about 0.58 dB at BER of 5×10^{-2}. Figure 8 shows the performance improvement of rotated and unrotated 8PSK uncoded and LDPC-coded systems. The performance improvement in the rotated uncoded system over the unrotated case is about 0.23 dB at BER of 1.3×10^{-1}. Similarly, for the LDPC-coded system the performance improvement is about 0.53 dB at a BER of 4×10^{-3}.

From the above results it is evident that constellation rotation in both uncoded and LDPC-coded systems results in a better performance over quasi-static uncorrelated Rayleigh fading channels.
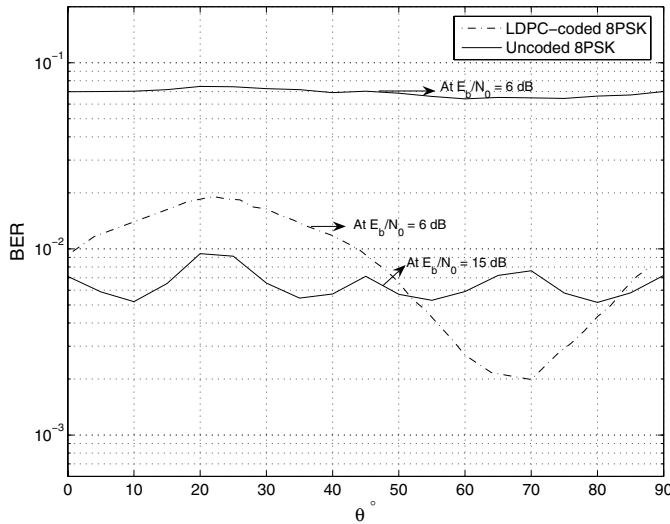
Fig. 6. BER performance of uncoded and LDPC-coded 8PSK systems with signal space diversity over different rotation angles.
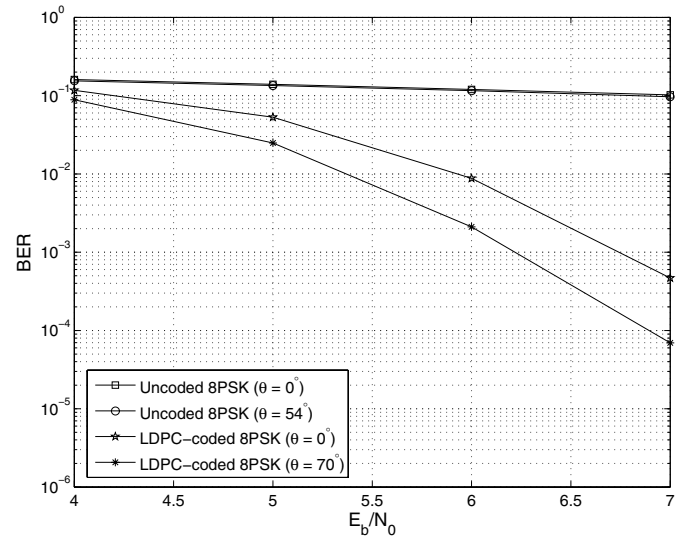

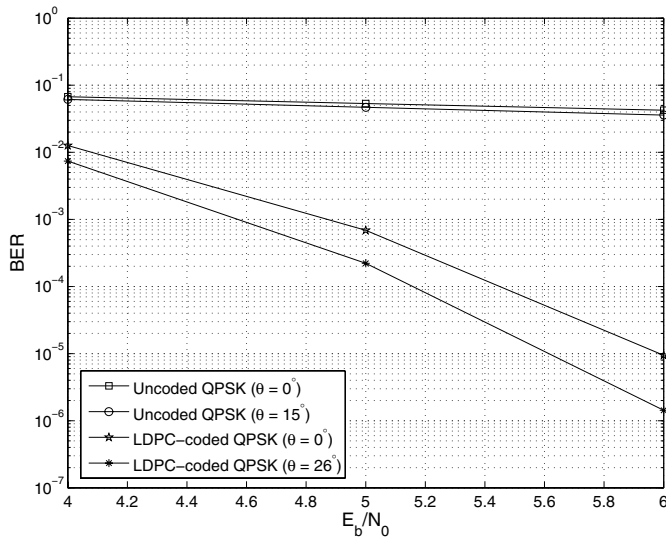Fig. 8. BER performance of uncoded and LDPC-coded 8PSK modulation schemes.

Fig. 7. BER performance of uncoded and LDPC-coded QPSK modulation schemes.

V. CONCLUSIONS

This paper presents the use of signal space diversity for multi-level modulation schemes in combination with LDPC coding. It was shown that under signal space diversity using MPSK constellations (uncoded or LDPC-coded) the system performance cannot be accurately evaluated by transmitting an all zero word (single symbol). It was found that LDPC-coded systems exhibit minimum BER performance at different rotation angles than the uncoded case. A proper choice of the constellation rotation in LDPC-coded systems leads to a significant performance improvement over the unrotated case in a system using signal space diversity over uncorrelated Rayleigh fading channels.

REFERENCES

[1] T. J. Richardson, M. A. Shokrollahi, and R. L. Urbanke, "Design of capacity approaching irregular low-density parity check codes," *IEEE Trans. Information Theory*, no. 47, pp. 619–637, Feb. 2001.
[2] J. Hou, P. H. Siegel, and L. B. Milstein, "Performance analysis and code optimization of low density parity-check codes on Rayleigh fading channels," *IEEE Journal on Selected Areas in Comm.*, vol. 19, no. 5, pp. 924–934, May 2001.
[3] C. Schlegel and D. J. Costello Jr., "Bandwidth efficient coding for fading channels: Code construction and performance analysis," *IEEE Journal on Selected Areas in Comm.*, vol. 7, no. 9, pp. 1356–1368, Dec. 1989.
[4] S. B. Slimane, "An improved PSK scheme for fading channels," *IEEE Trans. on Vehicular Tech.*, vol. 47, no. 2, pp. 703–710, May 1998.
[5] J. Boutros and E. Viterbo, "Signal space diversity: a power and bandwidth-efficient technique for the Rayleigh fading channel," *IEEE Trans. Information Theory*, vol. 44, no. 4, pp. 1453–1467, July 1998.
[6] A. Chindapol and J. A. Ritcey, "Design, analysis, and performance evaluation for BICM-ID with square QAM constellations in Rayleigh fading channels," *IEEE Journal on Selected Areas in Comm.*, vol. 19, no. 5, pp. 944–957, May 2001.
[7] X. Li and J. A. Ritcey, "Bit-interleaved coded modulation with iterative decoding and 8PSK signaling," *IEEE Trans. on Comm.*, vol. 50, no. 8, pp. 1250–1257, Aug. 2002.
[8] D. J. C. Mackay, "Good error correcting codes based on very sparse matrices," *IEEE Trans. Information Theory*, no. 2, pp. 399–431, Mar. 1999.
[9] B. Lu, G. Yue, and X. Wang, "Performance analysis and design optimization of LDPC-coded MIMO OFDM systems," *IEEE Trans. on Signal Process.*, vol. 52, no. 2, pp. 348–361, Feb. 2004.
[10] A. Stefanov and T. M. Duman, "Turbo coded modulation for systems with transmit and receive antenna diversity over block fading channels:system model, decoding approaches and practical considerations," *IEEE Journal on Selected Areas in Comm.*, vol. 19, no. 5, pp. 958–968, May 2001.